

Fermi-Bose mixture with tunable interactions

GIOVANNI MODUGNO

*LENS and Dipartimento di Fisica, Università di Firenze
Via Nello Carrara 1, 50019 Sesto Fiorentino, Italy*

1. – Introduction

The possibility of controlling the atom-atom interaction in ultracold quantum gases has recently opened various research directions, ranging from molecular physics in the nanoKelvin regime [1] to strongly interacting superfluid Fermi gases [2] and to strongly correlated atomic systems [3]. The interaction is usually controlled through Feshbach resonances [4], which consist in a resonant coupling of atomic and molecular levels that can be tuned through an external magnetic field.

This kind of tool has been extensively applied so far only to homonuclear Bose and Fermi systems. Tuning of the interactions in heteronuclear mixtures via Feshbach resonances can give access to an even broader range of phenomena. Interaction effects such as collapse or phase separation [5] would be accurately studied. A tunable interaction between the fermionic and bosonic components would also give access to a wealth of condensed-matter phenomena in strongly correlated systems that have been recently proposed [6]. Moreover, Feshbach resonances can be used to associate ultracold heteronuclear molecules. These would possess a permanent electric dipole moment, allowing to manipulate the samples via electric fields, and to study dipole-dipole interactions in the context of ultracold quantum gases. The presence of a long-range anisotropic interaction between the particles in Bose and Fermi quantum gases is expected to profoundly modify the properties of such systems, and to give access to new phenomenology [7, 8].

The study of Feshbach resonances in heteronuclear systems has been delayed by a few years with respect to the homonuclear case, mainly because of the larger complexity of the experiments and because of the lack of accurate theoretical models for Feshbach

resonances in most of the alkali pairs. Currently, Feshbach resonances have been experimentally detected in three alkali fermion-boson mixtures: ${}^6\text{Li}$ - ${}^{23}\text{Na}$ [9], ${}^6\text{Li}$ - ${}^7\text{Li}$ [10], ${}^{40}\text{K}$ - ${}^{87}\text{Rb}$ [11, 12]. However, a fine tuning of the interaction has so far been achieved only in the ${}^{40}\text{K}$ - ${}^{87}\text{Rb}$ system [13, 14].

In this work we first describe the various steps that have led to the observation of Feshbach resonances in the K-Rb system and their accurate characterization. We then describe recent experiments in which Feshbach resonances are exploited to study interaction effects and to perform first experiments on association of weakly bound KRb dimers.

2. – Feshbach resonances in the K-Rb mixture

Among ultracold Fermi-Bose atomic mixtures, the ${}^{40}\text{K}$ - ${}^{87}\text{Rb}$ system has so far been the most investigated one. Since its first production [15], it has been employed for a series of experiments on interaction phenomena and on Fermi and Bose gases in optical lattices. Nowadays it is by far the most employed ultracold atomic mixture. One of the peculiarities of this system that made it particularly interesting from the very beginning is the naturally attractive interaction between fermions and bosons. This is interesting to study mean-field effects such as collapse and bright solitons or boson-induced superfluidity. The possibility of tuning of the interspecies interaction via Feshbach resonances will further enlarge the spectrum of phenomena that can be investigated with this mixture.

Let us remind here a few general aspects of interactions in ultracold atomic gases and Feshbach resonances. The two-body interaction between atoms is described by a contact potential and the collisional events can be expanded in partial waves. At the low temperature of actual experiments, only the lowest order, energy-independent partial wave, i.e. the s -wave, need to be taken into account. Just one parameter, the s -wave scattering length a , is needed to define quantities such as the collisional cross-section and the coupling constant for interacting quantum gases in the mean-field approach. In a mixture of spin polarized fermions and bosons, two different interactions have to be considered: the fermion-boson interaction, described by a_{FB} , and the boson-boson one, described by a_{BB} . Fermion-fermion interaction must not be taken into account, since Pauli principle strictly forbids s -wave interaction between identical fermions. Throughout this work we consider the case in which only the interspecies scattering length a_{FB} can be tuned, while a_{BB} is fixed to its natural value (this is about $100 a_0$ for ${}^{87}\text{Rb}$). In general, the possibility of tuning at the same time both a_{FB} and a_{BB} in a fermion-boson system is marginal. The scattering length a_{FB} depends on the phase shift that the wavefunction of a pair of free atoms experiences when the pair separation approaches those typical of the molecular potential, i.e several tens of a_0 . As a matter of fact, the natural value of a_{FB} is determined just by the binding energy of the last vibrational state of the molecular potential. For example, in the case of the ${}^{40}\text{K}$ - ${}^{87}\text{Rb}$ pair in its ground state a_{FB} is negative and relatively large ($a_{FB}=-185 a_0$) because the closest molecular level to the atomic threshold is actually just above the threshold. By applying an external magnetic field to the system, it is possible to tune in a different way the energy of the atomic

threshold and that of the molecular states, and eventually obtain a situation in which a molecular level crosses the atomic threshold. At this crossing the scattering length of the system shows a resonant enhancement, the so called Feshbach resonance, and passes from $-\infty$ to $+\infty$ as the molecular state passes from above to below the atomic threshold. At one of such resonances, the magnetic field dependence of a_{FB} can be parametrized as

$$(1) \quad a_{FB}(B) = a_{bg}(1 - \Delta/(B - B_0)),$$

where a_{bg} is the background value of the scattering length, B_0 is the magnetic-field location of the resonance center, and Δ is a width parameter that accounts for the coupling strength of the specific atomic and molecular levels.

The ^{40}K - ^{87}Rb has a large number of internal states (the total angular momentum is $F=9/2$ for K and $F=1$ for Rb in their ground hyperfine state) and therefore in principle a large number of Feshbach resonances is available. In a series of experiments on cold collision measurements [16, 17, 18] we have determined to a good accuracy the scattering length a_{FB} of the system, which has been used to fine tune the best approximation of the K-Rb molecular potential, and in particular to determine the binding energy of the states close to dissociation. Actually, two different molecular potentials appear for alkali atoms, i.e. the singlet $X^1\Sigma^+$ and triplet $a^3\Sigma^+$ potentials with scattering lengths a_s and a_t , respectively. This study has then allowed to predict the magnetic-field position of Feshbach resonances [18]. In particular, for most of the states we expected several resonances in the region between 400 and 700 G. This prediction was confirmed by a first study of heteronuclear resonances in the absolute ground states performed at JILA [11]. In a successive detailed investigation of Feshbach resonances in various internal states [12] we got the complete picture of such resonances that is necessary for their exploitation in experiment. In the next section we describe the experimental and theoretical methods used.

3. – Feshbach spectroscopy

In our experiment the K-Rb Fermi-Bose mixture is routinely produced via laser and evaporative cooling in a magnetic trap [19, 15]. In order to study magnetic Feshbach resonances one has to decouple the trapping mechanism from the magnetic moment of the atoms. We achieved this by transferring the atoms from the magnetic trap to an optical dipole trap created by focused laser beams crossing in the horizontal plane. In a first series of experiments [12] we have used a titanium:sapphire laser at a wavelength of 830 nm, which is sufficiently detuned from the atomic resonance to provide a lifetime of the atomic sample exceeding 1 s. The trap depth was about $10 \mu\text{K}$, which is sufficiently large to hold "hot" samples at temperatures above quantum degeneracy. Typically 10^5 K fermions and 5×10^5 Rb bosons were cooled in a magnetic trap down to temperatures of a few hundreds nK and then adiabatically transferred to the optical trap. The typical density and temperature of the bosonic sample in the optical trap throughout this experiment were

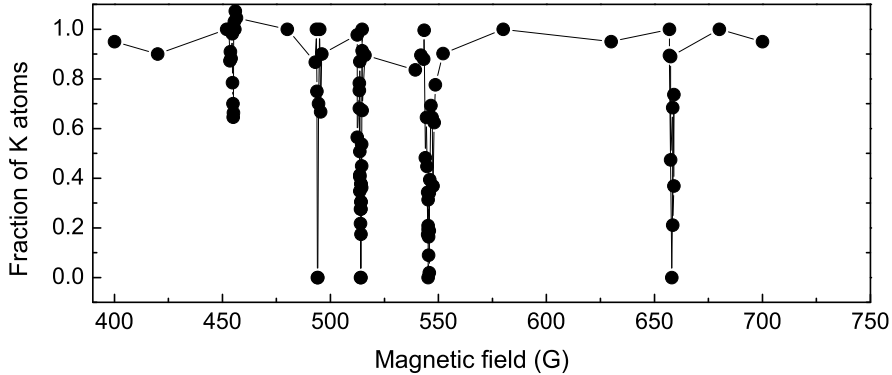


Fig. 1. – Relative inelastic losses of potassium atoms in a ^{40}K - ^{87}Rb mixture in its absolute ground state at interspecies Feshbach resonances. The two features near 456 G and 515 G are p -wave resonances, the others are s -wave resonances.

$5 \times 10^{12} \text{ cm}^{-3}$ and $1 \mu\text{K}$, respectively. The fermionic sample was in thermal equilibrium with the bosonic one.

The mixture was initially prepared in the state $|F^K = 9/2, m_F^K = 9/2\rangle \otimes |F^{Rb} = 2, m_F^{Rb} = 2\rangle$, which is the only stable combination of low-field seeking states. This state does not possess Feshbach resonances, since it has the maximum projection of the angular momentum. In the choice of a $\text{K} \otimes \text{Rb}$ state to explore for Feshbach resonances one has to take into account its stability against spin-exchange collisions. These are inelastic collisions which can take place every time a second state with the same projection of the total angular momentum $m_F^K + m_F^{Rb}$ with a lower energy is available. The excess kinetic energy is typically enough to have an immediate loss of the collision partners. Due to the particular level structure of this K-Rb mixture, all the states where both species are in their ground hyperfine state and either Rb or K are in their absolute ground state are stable against such collisions and have a lifetime that is limited mainly by three-body recombination. According to our theoretical study [18], most of these states were also expected to feature Feshbach resonances.

To prepare the atoms in these states we have used a series of radio-frequency (RF) and microwave (μw) adiabatic rapid passages. A first combination of sweeps was used to transfer the system to its ground state $|9/2, -9/2\rangle \otimes |1, 1\rangle$ in presence of a bias field of about 10 G. The field was then raised to 100 G to perform the additional transfer of K or Rb to excited states such as the $|9/2, -7/2\rangle$, $|9/2, 7/2\rangle$ or $|1, 0\rangle$.

The homogeneous field was then changed in few ms to any value in the range 0-1000 G and actively stabilized there with an accuracy of about 200 mG. The field was calibrated

by means of RF spectroscopy of the $|2, 2\rangle - |2, 1\rangle$ transition of Rb.

As we will describe in detail in the next section, a Feshbach resonance is usually accompanied by an enhancement of the inelastic decay rate. The easiest way to look for Feshbach resonances is therefore to record the fraction of atoms lost from the trap when changing the magnetic field. In our mixture the best sensitivity to resonances was achieved by recording the atom number of the minority component, i.e. potassium, after about 1 s of permanence at a fixed magnetic field. The typical experimental signature of interspecies resonance is shown in Fig. 1 for the absolute ground state of the mixture: due to the lower abundance of K in our sample, we usually observe a complete loss of K atoms at resonance. To avoid any possible confusion with homonuclear resonances we also check for the absence of losses after removing either K or Rb from the mixture before applying the magnetic field. Actually, in our investigation we have observed several Rb resonances that have been previously studied in dedicated experiments [20].

In a first survey we have detected 14 Feshbach resonances in three different states, and used them to refine our theoretical quantum collisional model. To do this, the singlet $X^1\Sigma^+$ and triplet $a^3\Sigma^+$ interaction potentials were parameterized in terms of the a_s and a_t scattering lengths, respectively. The two-body elastic cross section was then computed for different $a_{s,t}$ and its maxima, corresponding to Feshbach resonances, were compared to four sample experimental features. Once a good agreement was found, a least square fit to all 14 experimental features was then performed, letting also the van der Waals coefficient C_6 free to vary. The best fit parameters with one standard deviation we obtained are $a_s = (-111 \pm 5)a_0$, $a_t = (-215 \pm 10)a_0$ and $C_6 = (4292 \pm 19)$ a.u., which agrees to better than one standard deviation with the high precision *ab-initio* calculation obtained in [21]. Error bars also include a typical $\pm 10\%$ uncertainty in C_8 . The position and width of the resonances are listed in Table I. The average theory-experiment deviation for the resonance positions is about 0.3 G only.

A determination of the K-Rb scattering lengths based on extensive Feshbach spectroscopy is by far the most precise one can obtain. A large number of detected resonances indeed unequivocally maps the last few molecular states close to dissociation, and therefore determines the scattering lengths. Our determination of $a_{s,t}$ helped in solving some existing inconsistencies between previous experiments on cold collisions [17, 22], collapse [23, 24] and Feshbach resonances [11] in this mixture. The optimized ^{40}K - ^{87}Rb model can also be used to determine singlet and triplet scattering lengths for any K-Rb isotopic pair [12]. Within the Born-Oppenheimer approximation this can be simply achieved by using the appropriate reduced mass in the Hamiltonian. Such mass-scaling procedure depends in a sensitive way on the actual number of bound states supported by the potentials. They are nominally $N_b^s = 98$ and $N_b^t = 32$ for the singlet and triplet *ab initio* potentials we use, with an expected uncertainty of ± 2 [25]. Other quantities of general interest for experiments with K-Rb mixtures are the effective elastic scattering length a and the location of Feshbach resonances for the absolute ground state. We have determined also these quantities with relatively high accuracy using the collisional model above; they can be found in Ref. [12]. These data complete our previous investigation [16], and are of great interest for forthcoming experiments on Bose-Bose mixtures with K and Rb atoms

TABLE I. – *Magnetic-field positions and widths of the observed ^{40}K - ^{87}Rb resonances compared to the corresponding theoretical predictions of our best-fit model. Δ_{th} is defined in the text, and ℓ is the orbital angular momentum of the molecular state associated to each resonance.*

$ m_{fa}\rangle \otimes m_{fb}\rangle$	B_{exp} (G)	B_{th} (G)	$-\Delta_{\text{th}}$ (G)	ℓ
$ -9/2\rangle \otimes 1\rangle$	456.0	456.5	$2 \cdot 10^{-3}$	1
	–	462.2	0.067	0
	495.6	495.7	0.16	0
	515.7	515.4	0.25	1
	546.7	546.8	2.9	0
	547.4	547.6	0.08	2
	658.9	659.2	1.0	0
	663.7	663.9	0.018	2
$ -7/2\rangle \otimes 1\rangle$	469.2	469.2	0.27	0
	–	521.6	0.051	0
	584.0	584.1	0.67	0
	591.0	591.0	$2 \cdot 10^{-3}$	2
	598.3	598.2	2.5	0
	697.3	697.3	0.16	0
	705.0	704.5	0.78	0
	$ 7/2\rangle \otimes 1\rangle$	299.1	298.6	0.59
852.4		852.1	0.065	0

[26, 27].

Let us now discuss the properties of the Feshbach resonances we detect in the experiment, listed in Tab. I. The nature of the molecular states associated to the resonances can be better understood through multichannel bound state calculations. Since a_s and a_t are comparable the spacing between singlet and triplet vibrational levels is small compared to the hyperfine interaction. Strong singlet/triplet mixing then occurs at least for the two vibrational states closest to dissociation, resulting in molecular levels labeled as $(F^K F^{Rb} F \ell)$ in *zero* magnetic field, where ℓ is the rotational quantum number and $\vec{F} = \vec{F}^K + \vec{F}^{Rb}$. The features below ≈ 600 G arise from these strongly mixed levels. At such magnetic fields however the Zeeman magnetic energy is comparable to the smaller hyperfine splitting in the system, that of ^{40}K . Therefore F^K is not a good quantum number to label the resonances, whereas F^{Rb} is approximately good and equal to 2. Resonances at higher magnetic field correlate with more deeply-bound states and tend to assume singlet or triplet character. In all cases ℓ is an almost exact quantum number and is also shown in Tab. I.

The measurement of inelastic decay features described above allows to access only

the location of Feshbach resonance, but not the exact magnetic field dependence of the fermion-boson scattering length. This can be calculated by our collisional model: isolated resonances are well described by the simple parametrization introduced above: $a_{FB}(B) = a_{bg}(1 - \Delta_{th}/(B - B_0))$. The background scattering length for a particular state is determined by the model with an accuracy comparable to that obtained for $a_{t,s}$. For example, the determined value for the ground state is $a_{bg}=(-185\pm 7) a_0$. The width Δ_{th} can also be calculated for all resonances, and is shown in Tab. I, together with the angular momentum ℓ of the corresponding molecular states. The $\ell=0$ molecules tend to give rise to broad resonances due to strong spin-exchange coupling to incoming s -wave atoms. We also observe a few narrow resonances due to coupling of a $\ell=2$ molecule to incoming s -wave atoms through weaker anisotropic spin-spin interactions [28, 29]. The two resonances associated with $\ell=1$ molecules couple by spin-exchange to incoming p -wave atoms. These resonances have an energy-dependent width [30] which we compute at collision energy $E/k_B \approx 1\mu\text{K}$, with k_B the Boltzmann constant. Tab. I also shows two narrow not yet observed resonances. We find that several stable states of the mixture present at least one broad resonance, analogous to that in the ground state near 546 G. Any of these resonances can be very well suited for control of the interaction and molecule formation.

The resonance width can also be measured in the experiment by locating the so called zero-crossing, i.e. the magnetic-field value at which $a_{FB}=0$. For example, we have done this for one of the broadest resonances of our system by studying the efficiency of sympathetic cooling of fermions close to the resonance. A mixture composed by about 10^6 bosons and 10^5 fermions is loaded in a crossed dipole trap at a temperature around $1\mu\text{K}$. We performed this experiment using a Yb:YAG laser emitting at 1030 nm. We chose relatively large beam waist radii of about $100\mu\text{m}$, in order to have a relevant vertical sag of the rubidium cloud into the non-parabolic part of the optical trap. This resulted in a more efficient evaporation of Rb than of K when lowering the overall trap depth via acousto-optic modulators. Fig. 2 shows the temperature of the fermionic component after a 2.4 s evaporation in vicinity of the broad Feshbach resonance in the ground state located at 546.7 G. Thermalization to lower temperatures of spin-polarized fermionic atoms can take place only via efficient fermion-boson elastic collisions. Since the collisional cross-section at these low temperature is well described by $\sigma=4\pi a_{FB}^2$, it vanishes when a_{FB} crosses zero. The zero-crossing location extracted from a gaussian fit to the temperature of the fermionic component is 543.4(1) G. This gives a width $\Delta=3.3(2)$ G which is in good agreement with the theoretical expectation of $\Delta=3$ G. We have checked that such agreement between model and experiment persists on a few other broad resonances of the mixture.

4. – Three-body losses at a Feshbach resonance

The resonance in the ground state of the mixture around 546 G is in principle the most appropriate to achieve a fine tuning of the fermion-boson interaction. This is indeed one of the broadest resonances, and moreover it can be expected to have the slowest inelastic

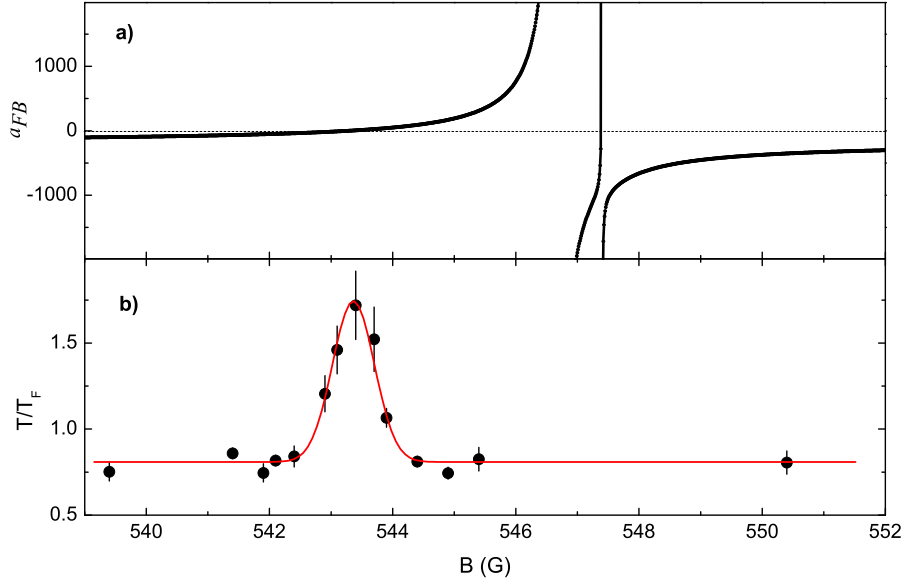


Fig. 2. – a) Theoretical expectation for the fermion-boson scattering length a_{FB} at the broadest Feshbach resonance in the ground state of the K-Rb mixture. b) Efficiency of sympathetic cooling of fermions around the zero-crossing location. The feature at 547.4 G is a narrow spin resonance.

decay achievable for this mixture. Two-body inelastic processes are indeed forbidden for the ground state, and only three-body recombination is responsible for decay in proximity of Feshbach resonances.

In a first series of experiments we have explored the main features of three-body recombination in our system in the thermal regime, in absence of possible interaction effects. At a boson-fermion Feshbach resonance, three-body processes involving two bosons and one fermion are the dominant decay channel, while those involving two fermions and one boson are suppressed by the Pauli principle [31]. During a three-body event, one boson and one fermion are associated into a deeply bound dimer whose binding energy is shared as kinetic energy by the dimer and the second boson. Conservation of energy and momentum require this energy to be shared by the KRb dimer and the Rb atom in a ratio of approximately 2:3. Typically this energy is at least of the order of $100\text{MHz} \times \hbar$, hence much larger than the trap depth, and both atom and dimer are immediately lost. In the regime of very large scattering lengths the loss rate is expected to depend on bosons and fermions density distributions n_B and n_F and on the interspecies scattering

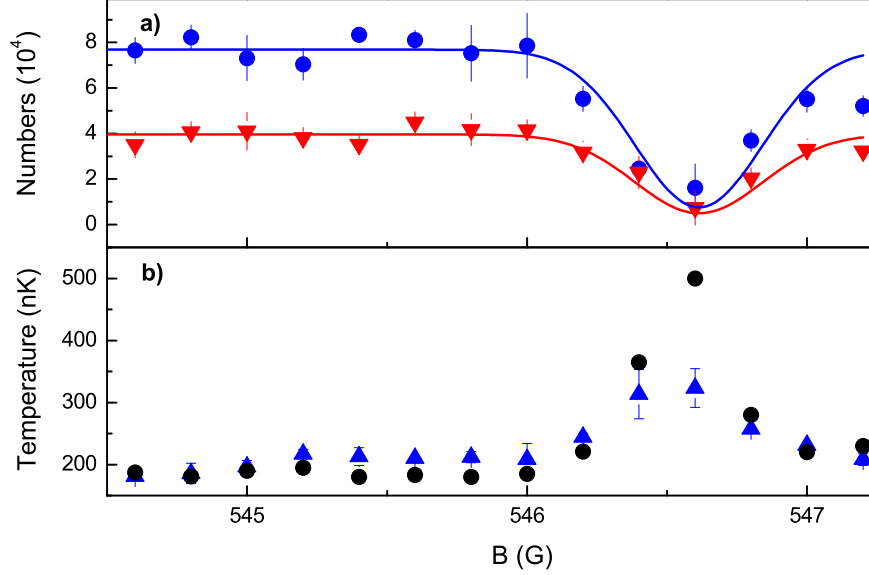


Fig. 3. – Three-body recombination in a thermal fermion-boson mixture after 100 ms of hold time at a Feshbach resonance. a) remaining atom number for fermions (triangles) and bosons (circles). b) final temperature for bosons measured in the experiment (triangles) and calculated (circles).

length as

$$(2) \quad \Gamma_3 = K_3 \int n_B^2(\mathbf{x}) n_F(\mathbf{x}) d\mathbf{x},$$

where $K_3 \propto a_{FB}^4$ [31]. In general, these losses result also in a heating of the remaining sample, since the probability of finding two bosons and one fermion in the same location is larger at the center of the distributions, where the coldest atoms reside [32]. The average energy per lost particle can be computed as

$$(3) \quad E_l = \frac{\int U(\mathbf{x}) n_B^2(\mathbf{x}) n_F(\mathbf{x}) d\mathbf{x}}{\int n_B^2(\mathbf{x}) n_F(\mathbf{x}) d\mathbf{x}},$$

where U is the potential energy of the trapped atoms. If the boson and fermion distributions are equal, one finds the same heating rate found for homonuclear bosonic systems: the energy per lost particle is $0.5k_B T$. This implies $3k_B T$ excess energy for each loss event, to be redistributed in the remaining sample.

In the experiment we have investigated the heating related to three-body losses. For example, Fig. 3 shows the evolution of atom numbers and temperature for a nondegenerate K-Rb sample that was held for 100 ms at various magnetic fields around 546 G. We clearly see a heating of the sample as the number of atoms drops close to the resonance. Here we compare the temperature measured in the experiment to the one calculated with an intuitive model. Such model evaluates the time-evolution of the mixture as a series of single three-body recombination events, each one followed by rethermalization at a higher temperature due to the $3k_B T$ excess energy. Experiment and theory are in qualitative agreement, although the latter slightly overestimates the heating.

5. – Tuning of the interaction in the quantum degenerate regime

When the sample is cooled into the quantum degenerate regime in proximity of the Feshbach resonance the properties of the system are largely modified by the resonant interaction between the two components. The Fermi-Bose interaction energy

$$(4) \quad U_{FB}(\mathbf{x}, a) = \frac{2\pi\hbar^2}{\mu} a_{FB} \int n_B(\mathbf{x}, a_{FB}) n_F(\mathbf{x}, a_{FB}) d\mathbf{x},$$

can get comparable or even much larger than the trap potential, and therefore determines the distributions of the two components in the trap [5]. In the case of $a_{FB} < 0$ the large attractive interaction can beat the natural repulsion within the Bose and Fermi gases and lead to a collapse of the system. For large $a_{FB} > 0$ the two components can instead undergo phase separation.

Collapse of a Fermi-Bose mixture has already been observed in this system as a sudden loss of a relevant fraction of the atoms when the number of atoms in the condensate was increased along the evaporation path [24]. The background K-Rb scattering length is indeed negative and sufficiently large to reach the unstable region for large atom numbers in tightly confining traps. No evidence of phase separation has instead been reported in mixtures with positive scattering length. The possibility of a rapid, fine tuning of the interaction at a Feshbach resonance allows to access and characterize both regimes of phase separation and collapse. In the experiment we have investigated these regimes through a study of three-body losses in the quantum degenerate regime. We indeed found that the loss behavior can give strong indications on the overlap of the two components in the trap.

To perform this experiment we produced a fully degenerate mixture by evaporative cooling in the crossed dipole trap at 1030 nm. The trap depth was lowered exponentially from 5 μ K to 0.5 μ K in 2.4 s, with a time constant of 1 s. The trap was then recompressed to the full depth in 150 ms. The trap frequencies for Rb were (120,92,126) Hz and a factor about $\sqrt{(87/40)}$ larger for K. The Fermi gas typically contains $5 \cdot 10^4$ atoms at a temperature $T < 0.3T_F$, where $T_F=500$ nK. The Bose-Einstein condensate contains instead about 10^5 atoms and no thermal component is discernible, i.e. the temperature is below 30 nK. The chemical potential of the Bose gas is $\mu/k_B=250$ nK. Due to the

different energy scale, the linear sizes of the Fermi gas are almost twice those of the Bose gas. The latter is totally contained in the volume of the Fermi gas, and is shifted down by about $7 \mu\text{m}$ by the larger gravitational force.

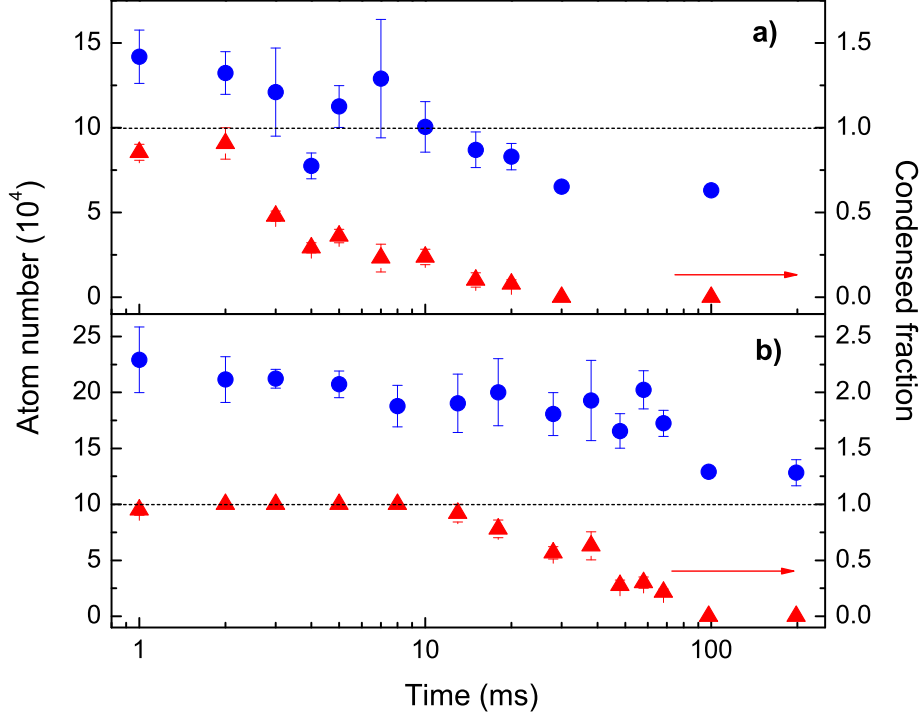


Fig. 4. – Time-evolution of the boson number (triangles) and of the condensed fraction (circles) for large positive and negative scattering lengths: a) $a_{FB} = -820^{+40}_{-40}$; b) $a_{FB} = +740^{+80}_{-70}$. In the first case the inelastic decay and heating is sped up by interaction-induced collapse; in the latter case it is slowed down by phase-separation.

In a first experiment we have compared the time evolution of the mixture for two values of the magnetic fields corresponding to opposite values of the fermion-boson scattering length: $a_{FB} \approx \pm 800 a_0$. They were obtained by preparing the mixture far from the resonance and then rapidly shifting the field to the final value. For the positive a_{FB} the mixture was prepared at 539 G and then brought to 546.0 G, where the expectation is $a_{FB} = +740^{+80}_{-70}$. It was instead prepared at 551 G for negative a and then brought to 547.6 G, where the expectation is $a_{FB} = -820^{+40}_{-40}$. In such way crossing of the resonance center during the rapid sweep was avoided. In Fig. 4 we show the evolution of the condensed fraction of the Bose gas, which is the most sensitive component of the mixture to excitations and perturbations. On the negative a_{FB} side we see a very rapid depletion

of the condensate on a timescale shorter than the trap period, while for positive a_{FB} the condensate remains stable for a much longer time interval. At a longer time in both cases the Bose gas is heated up into a pure thermal cloud. This however happens already at about 20 ms for negative a_{FB} , and only at about 100 ms for positive a_{FB} . During the whole time span, the total atom number in the bosonic sample decreases by about 50% in the case of negative a_{FB} and about 30% for positive a_{FB} . For the Fermi gas (not shown in the picture) we similarly observe both atom loss and heating, which are larger for negative a_{FB} .

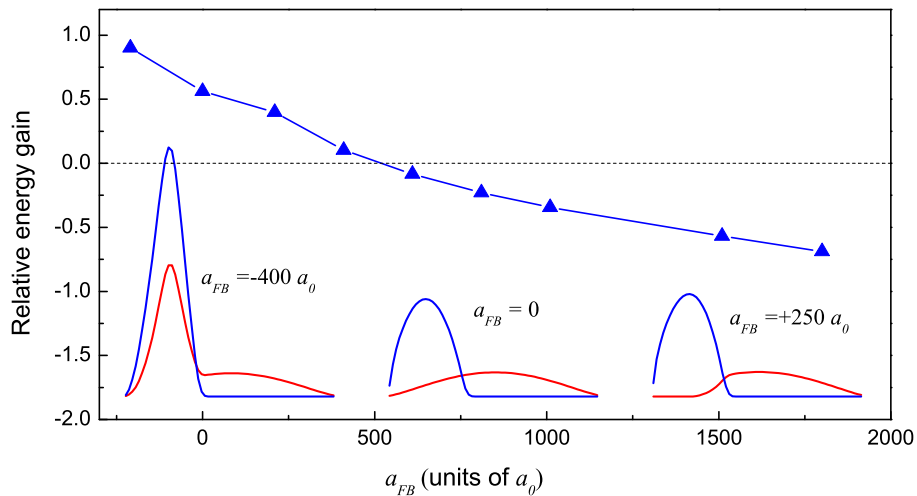


Fig. 5. – Calculated relative energy gain $(\overline{E}_B - E_l)/\overline{E}_B$ for each particle lost in a three-body collision event for a K-Rb Fermi-Bose mixture with variable interspecies interaction. For scattering lengths below $500 a_0$ the system energy increases as a consequence of losses, while above that value it decreases. This is a consequence of an increased overlap in the first case, and of phase separation in the second one, as shown by the calculated distributions along the vertical direction of bosons and fermions at $T=0$.

To understand the dramatically different behaviors observed for positive and negative a_{FB} s we rely on a zero-temperature mean-field model of our system [33]. We use it to study the density distribution of the mixture in the two regimes, and to predict the evolution of three-body losses. This model calculates the local interaction energy and uses it as an additional effective potential for both species to evaluate the distribution of the mixture in the trap. This procedure is done recursively until the true ground state of the system in presence of interaction is found.

For example, in Fig. 5 we plot a cut along the z direction of the distribution of the two components when the number of fermions and bosons is the same and equal to 5×10^4 , for

three different values of a_{FB} : 0, $-400 a_0$ and $+250 a_0$. In the case of large negative a_{FB} the density overlap of the two components is clearly increased with respect to the non-interacting case, while for large positive a_{FB} the two components tend to phase separate and it is strongly reduced. Note that the model would not converge for $a_{FB}=-800 a_0$, since the system is collapsed, i.e. it does not possess a stable ground state.

A reduced or increased overlap will obviously affect the three-body loss rate Γ_3 , which increases in the regime of collapse and is reduced in the phase-separation regime. This will affect the ratio between the mean energy of particles in the overlap region and the mean energy of the whole system, which determines the heating rate. We have used the model to calculate numerically the evolution of the overlap integral, the mean energy per lost particle and the mean energy per particle in the system, at $T=0$. For example, in Fig. 5 we show the excess energy per lost particle, normalized to the mean energy in the Bose condensate:

$$(5) \quad \frac{\overline{E}_B - E_l}{\overline{E}_B}, \quad \text{where: } \overline{E}_B = \frac{\int U(\mathbf{x})n_B(\mathbf{x})d\mathbf{x}}{\int n_B(\mathbf{x})d\mathbf{x}}.$$

For $a_{FB}=0$ the model predicts a relative energy gain of about 0.5, close to the classical value discussed above of $2/3$. The increase of heating on the $a_{FB} < 0$ side and the corresponding reduction on the $a_{FB} > 0$ side are apparent. Actually, this model indicates that three-body losses should eventually *cool down* the system as a_{FB} gets larger than $500a_0$, where the relative energy gain becomes negative.

Let us now interpret the behavior shown in Fig. 4 on the basis of the model's predictions. For $a_{FB} \approx -800a_0$ the system presumably starts a compression phase just after the interaction energy is switched to a large and negative value. After a quarter of the trap period, i.e. 2.5 ms, we have a maximum of three-body loss rate and a large heating of the sample. The condensate is therefore rapidly heated into a thermal cloud, and the loss rate decreases because of the decreased density of the samples. In the opposite case, $a_{FB} \approx +800a_0$, the system is in the phase-separation regime. For the first 100 ms the condensate is not heated up despite a 15% loss of atoms, indicating that high-energy atoms are preferentially removed by the loss events.

Note that in order to have a more realistic, quantitative description of the system's behavior, one would need a more complex model which can also track the dynamics of the system at finite T . For example, according to the simple model described above one would expect to see a cooling of the system as the loss process goes on. We think this is not observed because of the presence of the weakly bound molecular state on this side of the resonance that is responsible for the existence of the resonance itself. This can be expected to result in the production of just moderately energetic atom-molecule pairs, i.e. with a binding energy comparable to the trap depth. These would have time to scatter with the remaining atoms before leaving the trap, given the large collisional rate expected in this regime (of the order of 1000 s^{-1}).

The dramatically different behavior of losses on the two sides of the resonance appears also in the measurements reported in Fig. 6. Here we report the evolution of the Bose-

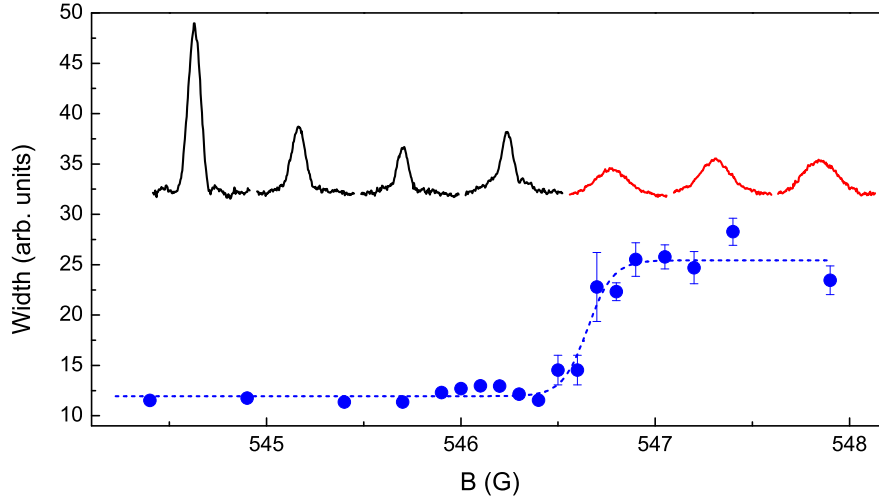


Fig. 6. – Evolution of the Bose-Einstein condensate in the mixture following a slow sweep across the Feshbach resonance from $a_{FB} > 0$ to $a_{FB} < 0$. Despite a strong reduction in the atom number due to three-body losses, the system remains stable until the field crosses the resonance center, where it is totally heated up into a thermal sample. A phenomenological fit of the gaussian width of the condensate with a Boltzmann growth function gives an accurate estimation of the resonance center.

Einstein condensate in the mixture following a sweep over the Feshbach resonance. The field was increased in 50 ms from $B_i=543.4$ G to a final field B that was varied from 543.4 G to 548 G, and held there for 10 ms. Inelastic losses start to deplete the system as the sweep approaches the resonance center, but the condensate survives as long as $a_{FB} > 0$. It is instead very rapidly destroyed by collapse when the sweep crosses the resonance center into the $a_{FB} < 0$ region. The evolution of the width of the gas after ballistic expansion with B can be used to find accurately the resonance center, as shown in Fig. 6b. A phenomenological fit with a Boltzmann growth function gives $B_0=546.65(20)$ G, which is in good agreement with the measured position of the loss maximum.

The possibility of a fine tuning of the interaction allows also to explore the threshold for the collapse instability in the region $a_{FB} < 0$. According to our mean-field model, the system is expected to remain stable as long as $a_{FB} > -400 a_0$, and to collapse for larger negative scattering lengths. Fig. 7 shows the evolution of the width of the Bose-Einstein condensate after a sweep from above the resonance into the instability region. The field was decreased in 50 ms from $B_i=551$ G to a lower final field B , and held there for 20 ms. The width of the condensate starts to increase around $B_f=549.4$ G until around $B_f=548.6$ G the condensate is totally heated into a thermal sample as a consequence of

collapse. In the highlighted region we observe a smooth transition between stable and unstable conditions: the condensate is heated up by three-body recombination and shows shape excitations due to the rapid change of the interaction energy. The corresponding scattering length range is $a_{FB} = -600 \div -350 a_0$ in qualitative accordance with the theory prediction.

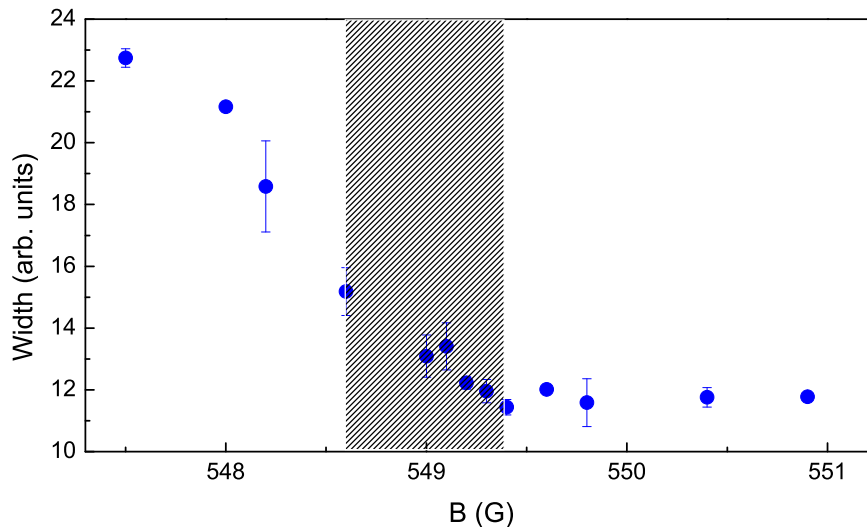


Fig. 7. – Evolution of the width of the Bose-Einstein condensate in the mixture following a sweep in the region of $a_{FB} < 0$ close to a Feshbach resonance. The highlighted area indicates the transition magnetic-field region from a stable to an unstable (collapsed) system.

Note that in this simple experiment it is difficult to make a more precise determination of the threshold scattering length. It is indeed difficult to separate an increase of the width due to a complete collapse of the system from an increase due to ordinary three-body losses in the regime of large attractive interactions or simply a modified expansion of the Bose gas in presence of the Fermi gas. Further investigation is needed in order to characterize the whole phenomenology and possibly test mean-field models of this system.

6. – Formation of dimers

An interspecies Feshbach resonance can also be exploited to associate pairs of atoms into KRb dimers, using the same technique that has proven successful in the case of homonuclear systems. The idea is simple: since the resonance takes place in coincidence with a crossing of an atomic and a molecular state, one can adiabatically convert pairs of

atoms into molecules with a magnetic-field sweep. The magnetic-field dependence of the atomic and molecular state involved in the resonance we studied are plotted in Fig. 8. The sweep needs to originate in the region $B > B_0$, where $E_a < E_m$, and end on the other side. A maximum ramp speed can be evaluated with a simple Landau-Zener model developed for homonuclear gases, which describes the number of molecules as

$$(6) \quad N_{mol} = N_{max}(1 - e^{-\delta_{LZ}}), \quad \text{where } \delta_{LZ} = \alpha n \Delta / \dot{B},$$

and $\alpha = 4.5(4) \times 10^4 \text{ m}^2 \text{s}^{-1}$ is an experimentally determined coupling constant [34]. The maximum conversion is reached when δ_{LZ} gets larger than one, which in our case corresponds to ramp speeds smaller than 50 G/ms.

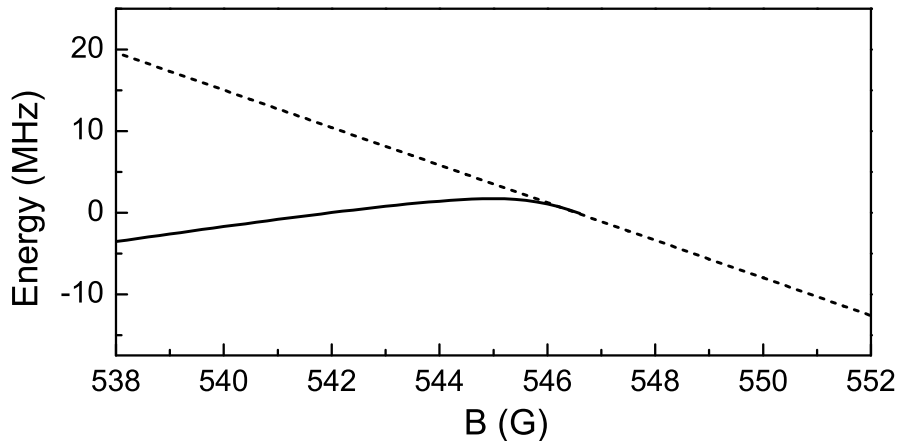


Fig. 8. – Magnetic-field dependence of the atomic (dashed line) and molecular (continuous line) states involved in the ground-state K-Rb Feshbach resonance. The atomic state is $|9/2, -9/2\rangle \otimes |1, 1\rangle$, while the molecular state is labeled as $F^{Rb}=2, \ell=0$, and has mixed singlet-triplet nature.

Fig. 9 shows a series of absorption images of the mixture taken at various intermediate magnetic fields during a sweep over the Feshbach resonances. The sweep was originating 4 G above the resonance, and ended after about 5 ms at a variable magnetic field across the resonance. The clouds were released from the optical trap right at the end of the sweep, and the images were taken at zero magnetic field, after an appropriate ballistic expansion. Note how the number of atoms in both components drops as the field is brought below 547 G. As in previous experiments, we interpret this reduction in atom numbers as the result of molecule formation. The transition energy of the molecules is indeed no longer resonant with the light used to image the atoms, and molecules are therefore not detected. It is important to note that the atoms are not lost because of

three-body recombination while sweeping over the resonance center, where $a_{FB} \rightarrow \pm\infty$. Indeed, in that case one would detect also a strong heating of the system, which is not apparent in Fig. 9.

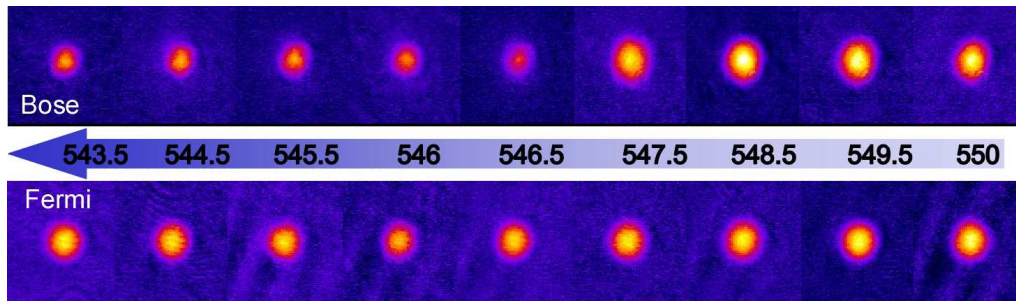


Fig. 9. – Evolution of the atom numbers in the mixture during a downward magnetic-field sweep at the ground-state Feshbach resonance. The sudden decrease in atom number for both components when the field crossed the resonance center at 546.6 indicates that atom pairs are associated into KRb dimers.

Qualitative information on the process of molecule formation in this system can be obtained through simple measurements. The maximum conversion efficiency we were able to observe is about 30-40%, that is not obtained at the lowest temperatures achievable in the experiment, but at temperatures around the condensation temperature of bosons T_c . This can be qualitatively understood in terms of the simple model and of the experiments on homonuclear systems presented in [34]. One expects to reach the maximum conversion efficiency when the phase space overlap of the two components is maximum. This is reached for $T=0$ in the homonuclear Fermi or Bose cases, but not for a Fermi-Bose system, where the spatial overlap of the two samples starts to decrease rapidly as soon as T gets smaller than T_c .

A crucial information for future experiments on such molecules is obviously the stability of the molecular sample. This can be investigated by reconvertng the molecules into atoms via a backward sweep across the resonance. We have been able to see molecules converted back into atoms only under special conditions: very short permanence on the molecular side of the resonance (shorter than $500 \mu\text{s}$), and very low number of unpaired bosonic atoms. This apparently indicates that the main decay channel of the molecular sample is inelastic collisions with free bosonic atoms. Further experiments in which one is able to remove the free atoms of both species will be helpful to give a quantitative assessment of this preliminary indication. A possible solution to the short lifetime of the molecular sample is also the use of a tight 3D optical lattice. This environment allows to prepare isolated K-Rb atomic pairs into individual lattice sites, allowing for a loss-free production of KRb molecules when sweeping over the resonance. As recently shown in experiments [35], this allows to have a lifetime exceeding 100 ms, although this is obtained at the expenses of a lower conversion efficiency.

7. – Outlook

In this contribution we have discussed experiment on a K-Rb Fermi-Bose mixture with tunable interaction at interspecies Feshbach resonances. The capability of controlling the boson-fermion scattering length to a high extent and the possibility of associating pairs of atoms into molecules open few different research directions.

The most important one is probably the study of ultracold dipolar molecules. Weakly bound KRb molecules produced at Feshbach resonances do not possess a relevant electric dipole moment, because their range is so large that only a negligible distortion of the electronic clouds is present. On the other hand, ground state ($X_1\Sigma^+$ ($\nu=0$)) KRb molecules are predicted to have a dipole moment of the order of 1 D [36]. These ground-state molecules can in principle be produced by transferring "Feshbach molecules" with optical Raman schemes [37] that are already being developed [38]. This is large enough to be used to investigate the fundamental properties of ultracold and quantum degenerate dipolar gases, and to test proposed schemes for quantum computing applications, in which electric fields are used to address and manipulate the particles [39]. The possibility of controlling at will the Fermi-Bose interaction will also allow to investigate novel quantum phases that have been proposed for strongly correlated atomic systems in optical lattices [6]. It can also allow to study in a more effective way the phenomenology of disordered systems [40]. Fine tuning of a_{FB} will also allow to test the predictions of present theories of Fermi-Bose systems for collapse [41] and phase-separation, collective excitations [42], effects beyond mean-field [43] and boson-induced superfluidity [44].

* * *

I thank Massimo Inguscio, a continuous source of ideas and encouragement, and Giacomo Roati, the driving force of the Fermi-Bose experiment at LENS. I also thank the other people that contributed to the work described in this lecture: Chiara D'Errico, Francesca Ferlaino, Michele Modugno, Andrea Simoni, and Matteo Zaccanti. This work was supported by MIUR, by EU under contract MEIF-CT-2004-009939, by Ente CRF, Firenze and by CNISM, Progetti di Innesco 2005.

REFERENCES

- [1] JOCHIM S., BARTENSTEIN M., ALTMAYER A., HENDL G., RIEDL S., CHIN C., HECKER DENSCHLAG J., and GRIMM R., *Science*, **302** (2003) 2101; GREINER M., REGAL C. A., and JIN D. S., *Nature*, **426** (2003) 537; ZWIERLEIN M., STAN C. A., SCHUNCK C. H., RAUPACH S. M. F., GUPTA S., HADZIBABIC Z., and KETTERLE W., *Phys. Rev. Lett.*, **91** (2003) 250401.
- [2] REGAL C. A., GREINER M., and JIN D. S., *Phys. Rev. Lett.*, **92** (2004) 040403; CHIN C., BARTENSTEIN M., ALTMAYER A., RIEDL S., JOCHIM S., HECKER DENSCHLAG J., and GRIMM R., *Science*, **305** (2004) 1128; BOURDEL T., *et al.*, *Phys. Rev. Lett.*, **93** (2004) 050401; PARTRIDGE G. B., *et al.*, *Phys. Rev. Lett.*, **95** (2005) 020404; ZWIERLEIN M. W., ABO-SHAER J. R., SCHIROTZEK A., SCHUNCK C. H., and KETTERLE W., *Nature*, **435** (2005) 1047.

- [3] WINKLER, K., *et al.*, *Nature*, **441** (2006) 853; STOFERLE, T., *et al.*, *Phys. Rev. Lett.*, **96** (2006) 030401; CHIN J. K., *et al.*, *Nature (London)*, **443** (2006) 961.
- [4] INOYUE S., *et al.*, *Nature (London)*, **392** (1998) 151.
- [5] MOLMER K., *Phys. Rev. Lett.*, **80** (1998) 1804.
- [6] ALBUS A., ILLUMINATI F., and EISERT J., *Phys. Rev. A*, **68** (2003) 023606; BÜCHLER H.P., BLATTER G., and ZWERGER W., *Phys. Rev. Lett.*, **90** (2003) 130401; LEWENSTEIN M., SANTOS L., BARANOV M. A., and FEHRMANN H., *Phys. Rev. Lett.*, **92** (2004) 050401.
- [7] BARANOV M. A., MARENKO M. S., RYCHKOV V. S., and SHLYAPNIKOV G.V., *Phys. Rev. A*, **66** (2002) 013606; DAMSKI B., *et al.*, *Phys. Rev. Lett.*, **90** (2003) 110401.
- [8] MICHELI A., BRENNEN G.K., ZOLLER P., *Nature Physics*, **2** (2006) 341.
- [9] STAN C. A., *et al.*, *Phys. Rev. Lett.*, **93** (2004) 143001.
- [10] ZHANG J., *et al.*, in *Proceedings of the XIX International Conference on Atomic Physics*, edited by L. G. MARCASSA, V. S. BAGNATO, and K. HELMERSON(AIP, New York) 2005.
- [11] INOYUE S., *et al.*, *Phys. Rev. Lett.*, **93** (2004) 183201.
- [12] FERLAINO F., D'ERRICO C., ROATI G., ZACCANTI M., INGUSCIO M., MODUGNO G., and SIMONI A., *Phys. Rev. A*, **73** (2006) 040702.
- [13] ZACCANTI M., D'ERRICO C., FERLAINO F., ROATI G., INGUSCIO M., and MODUGNO G., *Phys. Rev. A*, **73** (2006) 040702.
- [14] OSPELKAUS S., OSPELKAUS C., HUMBERT L., SENGSTOCK K., and BONGS K., *Phys. Rev. Lett.*, **97** (2006) 120403.
- [15] ROATI G., RIBOLI F., MODUGNO G. and INGUSCIO M., *Phys. Rev. Lett.*, **89** (2002) 150403.
- [16] FERRARI G., JASTREBSKI W., MODUGNO G., ROATI G., SIMONI A., and INGUSCIO M., *Phys. Rev. Lett.*, **89** (2002) 053202.
- [17] FERLAINO F., BRECHA R. J., HANNAFORD P., RIBOLI F., ROATI G., MODUGNO G., and INGUSCIO M., *J. Opt. B: Quantum Semiclass. Opt.*, **5** (2003) s3.
- [18] SIMONI A., FERLAINO F., ROATI G., MODUGNO G., and INGUSCIO M., *Phys. Rev. Lett.*, **90** (2003) 163202.
- [19] MODUGNO G., FERRARI G., ROATI G., BRECHA R., and INGUSCIO M., *Science*, **294** (2001) 1320.
- [20] MARTE A., *et al.*, *Phys. Rev. Lett.*, **89** (2002) 283202.
- [21] DEREVIANKO A., BABB J. F., and DALGARNO A., *Phys. Rev. A*, **63** (2001) 052704.
- [22] GOLDWIN J., INOYUE S., OLSEN M. L., NEWMAN B., DEPAOLA B. D., and JIN D. S., *Phys. Rev. A*, **70** (2004) 021601.
- [23] MODUGNO G., ROATI G., RIBOLI F., FERLAINO F., BRECHA R. J., and INGUSCIO M., *Science*, **297** (2002) 2200.
- [24] OSPELKAUS C., OSPELKAUS S., SENGSTOCK K. and BONGS K., *Phys. Rev. Lett.*, **96** (2006) 020401.
- [25] ZEMKE W. T., COTÉ R., and STWALLEY W. C., *Phys. Rev. A*, **71** (2005) 062706.
- [26] MODUGNO G., MODUGNO M., RIBOLI F., ROATI G. and INGUSCIO M., *Phys. Rev. Lett.*, **89** (2002) 190404.
- [27] CATANI J., MAIOLI P., DE SARLO L., MINARDI F., and INGUSCIO M., *Phys. Rev. A*, **73** (2006) 033415.
- [28] LEO P., WILLIAMS C. J., and JULIENNE P. S., *Phys. Rev. Lett.*, **85** (2000) 2721.
- [29] WERNER J., *et al.*, *Phys. Rev. Lett.*, **94** (2005) 183201.
- [30] TICKNOR C., REGAL C. A., JIN D. S., and BOHN J. L., *Phys. Rev. A*, **69** (2004) 042712.
- [31] D'INCAO J. P. and ESRY B. D., *Phys. Rev. A*, **73** (2006) 030702(R).
- [32] WEBER T., HERBIG J., MARK M., NÄGERL H.-C, and GRIMM R., *Phys. Rev. Lett.*, **91** (2003) 123201.
- [33] MODUGNO M., FERLAINO F., ROATI G., MODUGNO G., and INGUSCIO M., *Phys. Rev. A*, **68** (2003) 043626.

- [34] HODBY E., *et al.*, *Phys. Rev. Lett.*, **94** (2005) 120402.
- [35] OSPELKAUS C., *et al.*, *Phys. Rev. Lett.*, **97** (2006) 120402.
- [36] KOTOCHIGOVA S., JULIENNE P. S., and TIESINGA E., *Phys. Rev. A*, **68** (2003) 022501.
- [37] STWALLEY W. C., *Eur. Phys. J. D*, **31** (2004) 221.
- [38] WANG D., QI J., STONE M. F., NIKOLAYEVA O., WANG H., HATTAWAY B., GENSEMER S. D., GOULD P. L., EYLER E. E., and STWALLEY W. C., *Phys. Rev. Lett.*, **93** (2005) 243005; SAGE J. M., SAINIS S., BERGEMAN T., and DEMILLE D., *Phys. Rev. Lett.*, **94** (2005) 203001.
- [39] DEMILLE D., *Phys. Rev. Lett.*, **88** (2002) 067901.
- [40] GAVISH U. and CASTIN Y., *Phys. Rev. Lett.*, **95** (2005) 020401; GÜNTHER K., STHÖFERLE T., MORITZ H., KÖHL M., and ESSLINGER T., *Phys. Rev. Lett.*, **96** (2006) 180402; S. OSPELKAUS, *et al.*, *Phys. Rev. Lett.*, **96** (2006) 180403.
- [41] ADHIKARI S. K., *Phys. Rev. A*, **70** (2004) 043617.
- [42] LIU X.-J., MODUGNO M. and HU H., *Phys. Rev. A*, **68** (2003) 053605.
- [43] ALBUS A. P., ILLUMINATI F., and WILKENS M., *Phys. Rev. A*, **67** (2003) 063606.
- [44] HEISELBERG H., PETHICK C. J., SMITH H., and VIVERIT L., *Phys. Rev. Lett.*, **85** (2000) 2418; BIJLSMA M. J., HERINGA A., and STOOF H.T.C., *Phys. Rev. A*, **61** (2000) 052601; VIVERIT L., *Phys. Rev. A*, **66** (2002) 023605; MATERA F., *Phys. Rev. A*, **68** (2003) 043624.